ELSEVIER

Inorganica Chimica Acta 225 (1994) 57–66

Inorganica Chimica Acta

Electrochemistry of nitrite reductase model compounds 5. Electrochemistry and spectroelectrochemistry of iron porphinone, porphindione and isobacteriochlorin complexes

Yanming Liu, Michael D. Ryan

Chemistry Department, Marquette University, Milwaukee, WI 53233, USA

Received 11 June 1993

Abstract

The cyclic voltammetry and spectroelectrochemistry of iron complexes of porphinone, porphindiones and hydroporphyrins with alkyl substituents were carried out. Except for the alkyl isobacteriochlorin complexes, the half-wave potentials of the first ($Fe^{III}P/Fe^{II}P$), second ($Fe^{II}P/FeP^{-}$) and third (FeP^{-}/FeP^{2-}) waves were independent of the macrocycle identity. Any small differences were generally consistent with known substituents effects on the redox potentials. The half-wave potential of the second and third waves of iron isobacteriochlorin, Fe(2,4-DMOEiBC), (2,4-DMOEiBC = 2,4-dimethyloctaethylisobacteriochlorin), though, occurred at potentials significantly more negative than the porphyrin analogue. The second wave of Fe(2,4-DMOEiBC) occurred at −1.62 V versus SCE compared to −1.26 V for Fe(OEP). Similarly, the half-wave potential for the third wave was −2.15 V versus −1.83 V for Fe(OEP). This work is in contrast with previous work on iron tetraphenylporphyrin (FeTPP) and iron tetraphenylisobacteriochlorin (FeTPiBC), where the FeP/FeP^{-} half-wave potential was independent of macrocycle identity. The voltammetry of Fe(2,4-DMOEiBC)(Cl) in the presence of substituted pyridines was also examined. The macrocycle identity had no measurable effect in the formation constants of $Fe^{II}(P)$ with pyridines, β_2^{II}, while there was a systematic increase in β_2^{III} ($Fe^{III}(P)(Cl)$ with pyridines) with increasing saturation of the macrocycle. This indicates that the Lewis acidity of the ferric complex increased with macrocycle saturation. The spectroelectrochemical reduction of iron complexes with porphyrin, chlorin, isobacteriochlorin, porphinone and porphindione was also carried out. The formation of $Fe(P)^{-}$ from $Fe^{II}(P)$, where P = MOEC (methyloctaethylchlorin), led to a decrease in the molar absorptivity of the Soret band, as was observed for $Fe(OEP)^{-}$, as well as an increase in the number of bands (355, 411 and 456 nm). Three Soret bands were also observed for $Fe(OEPone)^{-}$, but these bands appeared as shoulders in $Fe(2,4\text{-}OEPdione)^{-}$ (OEPone = octaethylporphinone; OEPdione = octaethylporphindione). By contrast, the spectrum for $Fe(2,4\text{-}DMOEiBC)^{-}$ was quite different from $Fe(OEP)^{-}$, and was much more similar to the analogous complex, $Fe(TPiBC)^{-}$ (TPiBC = tetraphenylisobacteriochlorin). The Soret band absorbance decreased only a small amount and no new bands in the Soret region were observed. The visible spectra of Fe(2,4-DMOEiBC) and $Fe(2,4\text{-}DMOEiBC)^{-}$ were quite similar to isobacteriochlorin complexes with nickel and copper. In those complexes, the changes in the visible spectra upon reduction were explained on the basis of d_π to e_g^*-like backbonding. The oxidation of Fe(2,4-DMOEiBC)(Cl) caused a small decrease in the absorbance of the Soret band and a bleaching of the long wavelength band. The spectrum of $Fe(2,4\text{-}DMOEiBC)(Cl)^{+}$ had the same features as the previously reported superoxidized *E. coli* sulfite reductase.

Keywords: Electrochemistry; Iron complexes; Porphinone complexes; Porphindione complexes; Isobacteriochlorin complexes

1. Introduction

The amount of dinitrogen, nitrous oxide, ammonia, nitrite and nitrate on the earth is regulated by the nitrogen cycle [1]. One of the important steps in this cycle is the synthesis of ammonia from the reduction of nitrite, which is catalyzed by the enzyme assimilatory nitrite reductase. The prosthetic group in assimilatory nitrite reductase has been identified as an iron isobacteriochlorin, siroheme [2]. A second class of enzymes, called the dissimilatory nitrite reductases, which have either iron or copper as their prosthetic group, reduces nitrite to nitric or nitrous oxide. One of the iron enzymes contains four hemes, two hemes c and two hemes d_1, while another iron nitrite reductase is a hexaheme c enzyme (product is ammonia for this enzyme) [3]. Heme

SSDI 0020-1693(94)04029-U

d_1, which was also found to be an unusual porphyrin, has been shown to be an iron 2,4-porphindione [4].

The presence of these unique prosthetic groups in nitrogen metabolism has sparked considerable interest in recent years. Many research groups have examined the redox properties of isobacteriochlorin and porphindione complexes in order to investigate chemical differences due to the structure of the macrocycle [5–11]. The synthesis of these complexes was initially quite difficult due to their poor yield, stability and purity [12,13]. Recent advances, especially for the generation of porphinone and porphindione (heme d_1 model) from octaethylporphyrin by osmium tetroxide-oxidation [14,15], have simplified this work. The ketones groups on the porphinone or porphindione ligands can then be transformed to methyl-substituted chlorin and isobacteriochlorins (siroheme model) in high yield [16]. These materials do not undergo dehydrogenation, unlike the isobacteriochlorins which are generated by a formal hydrogen reduction [17,18]. The structures of the chlorin and isobacteriochlorin that are the focus of most of this work are shown in Fig. 1. The structures of other isobacteriochlorin and porphindione isomers are given in Refs. 16 and 19.

Voltammetric studies of free-base hydrophorphyrins [5,20–24], free-base porphinone and porphindiones [8,19], their iron complexes [5,6,8,11,17,25], and other metals [6,19,21,23,24] have been carried out. Only four of these reports, though, examined the electrochemistry of these ligands and complexes beyond the first reduction wave [11,19,21,25]. Low oxidation state iron porphyrins are unstable in the presence of alkyl halides [26], which makes it difficult to study these complexes in methylene chloride. Greater stability for the low oxidation states of iron porphyrins can be obtained in THF [27], and this fact was exploited recently in the study of iron tetraphenylchlorin (Fe(TPC)) and tetraphenylisobacteriochlorin (Fe(TPiBC)) [11]. Unfortunately, the tetraphenyl derivatives were quite unstable towards dehydrogenation, especially when the complexes were oxidized.

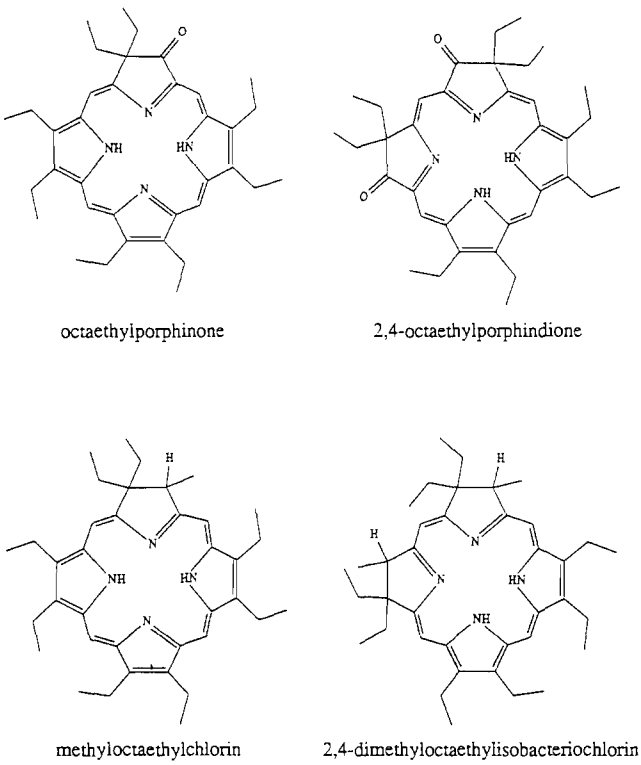

Fig. 1. Molecular structures for the hydroporphyrins, porphinone and porphindione used in this work.

Visible spectroelectrochemistry has been shown to be a convenient method for investigating the stability and spectral properties of low oxidation state compounds. Some examples include the spectroelectrochemistry of bonellin, a chlorin compound [22], palladium [28], copper [28], nickel complexes of porphyrins [29], hydroporphyrins [29] and porphindione [30], and the oxidation of Zn(OEiBC) [21] and a number of metal porphyrins [31,32]. A recent report from this laboratory has utilized this technique for the study of Fe(TPC) and Fe(TPiBC) [11]. In this work, oxidation of the iron hydroporphyrin complexes led to a facile dehydrogenation reaction and, hence, to chlorin or porphyrin complexes. While considerable progress was made studying the tetraphenyl derivatives, the poor stability of these hydroporphyrins has limited their utility. In this work, the more stable methyloctaethylchlorin (MOEC) and dimethyloctaethylisobacteriochlorin (DMOEiBC) will be used as the hydroporphyrin macrocycle. For comparison to heme d_1 models, porphinone (OEPone) and porphindione (OEPdione) will also be examined.

2. Experimental

2.1. Equipment

Cyclic voltammograms were obtained with an IBM Instrument EC/225 voltammetric analyzer with a Hewlett-Packard 7045A X-Y recorder. An Ag/0.1 M $AgNO_3$ (in acetonitrile) reference electrode was used; the potentials obtained were 0.456 V negative of the values that would have been recorded using an SCE ($E_{SCE} = E_{Ag/AgNO_3} + 0.456$ V). For comparison with literature values, this correction factor has been applied to all tabular data. A home-made cell with a solution volume of 2–4 ml was used in this work. The working and auxiliary electrodes were platinum. The UV–Vis spectra were recorded on a Hewlett-Packard 8452A diode array spectrophotometer or a Perkin-Elmer 320 UV–Vis spectrophotometer (for the spectroelectrochemical data). An optically transparent thin layer

electrochemical (OTTLE) cell was used for the spectroelectrochemical experiments [33].

2.2. Chemicals

Octaethylporphyrin (H_2OEP) was purchased from Aldrich Chemical Co. The hydroporphyrin, porphinone and porphindione ligands were synthesized by literature procedures [14–16] with slight modification. Porphinone, and 2,3-, 2,4- and 2,6-octaethylporphindione (H_2(OEPdione)) ligands were synthesized by osmium tetroxide oxidation [14,15]. In our hands, the purification of the crude products was not effective on silica gel, but pure products were obtained by separation of their respective zinc complexes on an alumina column. The iron complexes were made by reacting ferrous acetate with the appropriate macrocycle in acetic acid [17]. The methylated hydroporphyrins (methyloctaethylchlorin (H_2MOEC), dimethyloctaethylisobacteriochlorin (H_2DMOEiBC) and dimethyloctaethylbacteriochlorin (H_2DMOEBC) were synthesized from their respective porphinone or porphindione using literature procedures [16]. The iron complexes were synthesized in the same manner as the porphinone or porphindione complexes. Under these conditions, the ferric bacteriochlorin complex was not formed. The visible spectral data are summarized in Table 1.

2.3. Procedures

All solutions were deoxygenated by deaerating the solution for 15 min with prepurified dinitrogen. The dinitrogen was pre-saturated with the solvent in order to prevent evaporation. The spectroelectrochemical data were obtained after the current had decayed to the background.

The formation constants for the bis(pyridine)iron(II) complexes, β_2^{II}, were obtained from the shift in the potential of the second wave, as measured by differential pulse polarography, using Eq. (1) [34]

$$\log \beta_2^{II} = (\Delta E_p/0.059)/M_{py}^2 \quad (1)$$

where $\Delta E_p = E_{pu} - E_{pc}$, M_{py} is the bulk concentration of pyridine, and E_{pu} and E_{pc} are the differential pulse polarographic peak potentials of the second reduction wave in the absence and presence of the substituted pyridines, respectively. The $\log \beta_2^{II}$ values were calculated over a range of pyridine concentrations in order to verify that $Fe(P)^-$ did not complex with pyridine. The ratio of the formation constants for $Fe(P)(py)_2^+$, β_2^{III}, to β_2^{II} can be determined from the $E_{1/2}$ value of the first wave, as measured by cyclic voltammetry, using Eq. (2)

$$\log (\beta_2^{III}/\beta_2^{II}) = \Delta E_{1/2}/0.059 \quad (2)$$

where $\Delta E_{1/2} = E_{1/2,u} - E_{1/2,c}$, and $E_{1/2,u}$ and $E_{1/2,c}$ are the half-wave potentials of the iron(III)/iron(II) wave without and with pyridine present, respectively. The formation constants, β_2^{III} and β_2^{II}, refer to reactions (3) and (4)

$$Fe^{III}(P)(Cl) + 2py \rightleftharpoons Fe^{III}(P)(py)_2^+ + Cl^- \quad (3)$$

$$Fe^{II}(P) + 2py \rightleftharpoons Fe^{II}(P)(py)_2 \quad (4)$$

3. Results and discussion

3.1. Cyclic voltammetry of iron hydroporphyrins, porphinone and porphindiones

The cyclic voltammetry of iron complexes with porphyrin, hydroporphyrins, porphinone and porphindiones

Table 1
Visible spectral data for ferric hydroporphyrin, porphinone and porphindione complexes

Complex	Solvent	Soret band[a] (nm)	Other visible bands (nm) (ϵ (cm^{-1} $M^{-1} \times 10^{-3}$))
Fe(OEPone)(Cl)	THF	386 (66)	482 (8.3), 546 (6.6), 596 (14), 658 (3.5), 730 (3.6)
	CH_2Cl_2	390 (68)	482 (12), 508s, 550 (9.7), 600 (16), 662 (5.7), 742 (6.0)
Fe(2,3-OEPdione)(Cl)	THF	408 (39)	582 (7.7), 640 (11), 734 (6.8)
Fe(2,4-OEPdione)(Cl)	THF	376 (47), 418 (48)	524 (13), 568 (13), 600 (14), 668 (5.7), 722 (5.8)
	CH_2Cl_2	378 (69), 402s	526 (16), 574 (16), 612 (20), 676s, 756 (4.4)
Fe(MOEC)(Cl)	THF	376 (146)	472 (19), 508 (15), 558 (16), 602 (44), 672 (8), 754 (10)
Fe(2,3-DMOEiBC)(Cl)	THF	378	478, 508, 546, 598, 682, 752
Fe(2,4-DMOEiBC)(Cl)	THF	378 (102)	482 (20), 516 (20), 552 (21), 600 (39), 684 (5.1), 754 (4.8)

[a](ϵ, cm^{-1} $M^{-1} \times 10^{-3}$).

Table 2
Half-wave potentials for the oxidation and reduction of iron porphyrins, hydroporphyrins, porphinones and porphindiones

Complex	Solvent	$FeP(Cl)^+/FeP(Cl)$ $E_{1/2,o}$ (V)	$Fe^{III}P/Fe^{II}P$ $E_{1/2,1}$ (V)	FeP/FeP^- $E_{1/2,2}$ (V)	FeP^-/FeP^{2-} $E_{1/2,3}$ (V)	Ref.
Fe(OEP)(Cl)	THF	1.19[a]	−0.45[a]	−1.26[a]	−1.83[a]	tw[b]
	CH_2Cl_2	1.01	−0.52			[17]
Fe(OEC)(Cl)	CH_2Cl_2	0.72	−0.44			[17]
Fe(MOEC)(Cl)	THF	0.85[a]	−0.41[a]	−1.26[a]	−1.83[a]	tw
	CH_2Cl_2		−0.40[a]	−1.25[a,c]		tw
Fe(OEiBC)(Cl)	CH_2Cl_2	0.43	−0.45			[17]
Fe(2,4-DMOEiBC)(Cl)	CH_2Cl_2	0.44	−0.4			[6]
	CH_2Cl_2	0.47[a]	−0.43[a]	−1.49[a,c]		tw
	THF	0.56[a]	−0.42[a]	−1.62[a]	−2.15[a,c]	tw
Fe(2,3-DMOEiBC(Cl)	THF	0.57[a]	−0.45[a]	−1.68[a]		tw
Fe(OEPone)(Cl)	CH_2Cl_2	0.95	−0.34			[8]
	THF	1.02[a]	−0.35[a]	−1.23[a]	−1.83[a]	tw
Fe(2,3-OEPdione)(Cl)	THF	0.93[a]	−0.13[a]	−1.02[a]	−1.63[a]	tw
Fe(2,4-OEPdione)(Cl)	THF	0.96[a]	−0.16[a]	−1.15[a]	−1.55[a]	tw
	CH_2Cl_2	0.98[a]	−0.09[a]	−0.91[a,c]		tw
	CH_2Cl_2	0.84	−0.24			[8]

[a]Data were obtained vs. $Ag/AgNO_3$ reference electrode. For comparison to literature values, 0.456 V were subtracted from the data to obtain the values versus SCE. All data in Table 2 are versus SCE.
[b]tw = this work.
[c]Irreversible wave, E_p value used.

is summarized in Table 2. In the absence of excess chloride, the first reduction wave was quasi-reversible to irreversible. The wave was reversible in the presence of a small amount of chloride ion due to the acceleration of the complexation reaction, as had been reported earlier [35]. All potentials in Table 2 were measured under conditions so that the reversible potentials could be obtained, except as noted. As had been previously observed, there were no significant differences between the half-wave potentials of the first reduction wave, $E_{1/2,1}$, of Fe(OEP)(Cl) (−0.45 V) and Fe(OEiBC)(Cl) (−0.42 V) [5]. The $E_{1/2,1}$ values of Fe(OEPone)(Cl) and Fe(2,4-OEPdione)(Cl) were 100 and 300 mV positive of Fe(OEP)(Cl), respectively. The first oxidation wave, $E_{1/2,o}$, was also consistent with previous work, though the oxidations in THF were more difficult than in methylene chloride. As expected, the $E_{1/2,o}$ values shifted in the negative direction as the porphine ring became more saturated. Unlike the tetraphenyl derivatives, there was no evidence of macrocycle oxidation on the voltammetric timescale (i.e. the second wave for Fe(MOEC)(Cl) did not correspond to the first wave of Fe(OEP)(Cl)) [11].

Unlike the $E_{1/2,1}$ values, the half-wave potential for the second and third reduction ($E_{1/2,2}$ and $E_{1/2,3}$, respectively) did depend upon the identity of the macrocycle (Fig. 2). For the isobacteriochlorin complexes, the half-wave potentials shifted to more negative potentials compared to the iron porphyrin complex, while the shift was slightly positive for the iron porphinones and porphindiones [8]. For example, the half-wave potential for the second wave of Fe(2,4-DMOEiBC)(Cl)

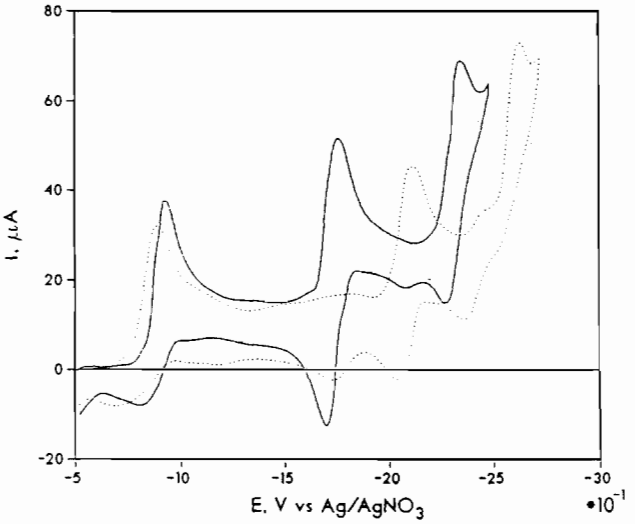

Fig. 2. Cyclic voltammetry of Fe(OEP)(Cl) (solid line) and Fe(2,4-DMOEiBC)(Cl) (dotted line) in THF at 100 mV/s. Working electrode: mercury; auxiliary electrode: platinum; reference electrode: $Ag/AgNO_3$ (0.1 M in acetonitrile); supporting electrolyte: 0.10 M TBAP.

occurred in THF at −1.62 V, compared to −1.26 V for Fe(OEP)(Cl), while the same wave for Fe(2,4-OEPdione)(Cl) occurred at −1.15 V. These results are in contrast with the iron tetraphenylporphyrin and hydroporphyrin voltammetry [11]. In this case, the second reduction wave did not depend upon the degree of saturation of the macrocycle. The irreversibility of the second wave in methylene chloride is probably due to the reaction of iron(I) with the solvent [26]. The same variation in half-wave potential (E_p values for

the irreversible waves) was observed for the third reduction wave. The third wave, while irreversible at slow scan rates for Fe(2,4-DMOEiBC)(Cl), became more reversible at higher scan rates, with the appearance of an anodic peak. This indicated that a slow irreversible reaction following the electron transfer occurred, and that, at the scan rates used, the E_p value was not far removed from its reversible position.

The variation in the $E_{1/2}$ values as a function of macrocycle identity for a variety of metals has been summarized in Table 3. For those processes that have been shown to be clearly porphine-centered (Fe^{III}-π-cation radical/Fe^{III}, Zn(II) and Pd(II) reduction), the half-wave potential of the metal complex could be predicted quite reasonably from the variation in the porphine potential (see Table 3). For those processes that were clearly metal centered, the $E_{1/2}$ values did not depend upon the identity of the macrocycle (Fe(III)/Fe(II), Fe^{II}(NO) reduction). The structure of the complex formed by the reduction of Ni^{II}(P) [29,37] and Cu^{II}(P) [28,38,39] has been shown in the literature to depend upon the identity of the macrocycle. In both these cases, the porphyrin and chlorin complexes are $M(P^{\cdot -})$, while the isobacteriochlorin complex is $M^{I}(P)^{-}$. For the iron complex, the $E_{1/2,2}$ and $E_{1/2,3}$ did depend upon the identity of the macrocycle, yet it is known that this reduction is already metal-centered when P = porphyrin [40]. These results indicate, though, that the isobacteriochlorin ligand is not able to stabilize the 'iron(I)' and 'iron(0)' complexes as well as the porphyrin and chlorin macrocycles.

3.2. Spectroelectrochemistry of the iron complexes

The first two reduction steps of Fe(OEP)(Cl), Fe(MOEC)(Cl), Fe(2,4-DMOEiBC)(Cl), Fe(OEPone)-(Cl) and Fe(2,4-OEPdione)(Cl) were monitored by visible spectroelectrochemistry in order to characterize the redox products. Isosbestic points were obtained during both reductions for all the complexes. The spectra of Fe(P) and $Fe(P)^{-}$, where P = MOEC and 2,4-DMOEiBC, are shown in Figs. 3 and 4, respectively, and the spectral data for all the complexes are summarized in Table 4. The chemical reversibility for the first two reductions was confirmed by returning the potential to the initial potential, where the ferric complex was stable. In all cases, the visible spectra showed the complete regeneration of the starting compounds. The addition of the first electron to the Fe(P)(Cl) complex led to a red shift (18–35 nm) in the Soret band, as well as an increase in absorbance, which are characteristic of the formation of an Fe(II) complex in THF. Only a single Soret band was observed for Fe(OEP) and Fe(MOEC), while a shoulder at shorter wavelengths was present for Fe(EOPone). For Fe(2,4-DMOEiBC) and Fe(2,4-OEPdione), the Soret bands were split. Where comparisons could be made, the results were consistent with previous work [43].

The spectral changes caused by the addition of a second electron into the complex depended upon the identity of the macrocycle. The formation of $Fe(OEP)^{-}$, $Fe(MOEC)^{-}$ (Fig. 3), and, to a lesser extent, the $Fe(OEPone)^{-}$ or $Fe(OEPdione)^{-}$ complexes, led to a significant attenuation and splitting of the Soret band,

Table 3
Variation in half-wave potentials as a function of macrocycle structure

Complex (oxidized form)	Macrocycle	Solvent	$E_{1/2}$ values (V)				Ref.
			Porphyrin	Chlorin	BC	iBC	
H_2-π-cation	OEP	THF	1.05[a]	0.82[a,b]	0.49[a]	0.57[a,c]	tw[d]
H_2	OEP	THF	−1.34[a]	−1.37[a,b]	−1.37[a]	−1.66[a,c]	tw
H_2-π-anion	OEP	THF	−1.70[a]	−1.70[a,b]		−2.12[a,c] irr	tw
Fe^{III}-π-cation	OEP	THF	1.19[a]	0.85[a,b]		0.44[a,c]	tw
Fe^{III}	OEP	THF	−0.45[a]	−0.41[a,b]		−0.42[a,c]	tw
Fe^{II}	OEP	THF	−1.26[a]	−1.26[a,b]		−1.68[a,c]	tw
Fe^{II}	TPP	THF	−1.07	−1.13		−1.14[e]	[36]
Fe^{I}	OEP	THF	−1.83[a]	−1.83[a,b]		−2.15[a,c]	tw
Fe^{II}(NO)	TPP	THF	−0.93	−0.90		−0.92	[11]
Cu^{II}	OEP		−1.47	−1.44		−1.50	[28]
Zn^{II}	TPP		−1.35	−1.33	−1.28	−1.73	[5]
Pd^{II}	OEP		−1.46	−1.44		−1.79	[28]
Ni^{II}	OEP		−1.50	−1.46, −1.48[b]		−1.54, −1.63[c]	[37]

[a]Data were obtained vs. $Ag/AgNO_3$ reference electrode. For comparison to literature values, 0.456 V were subtracted from the data to obtain the values vs. SCE.
[b]Methyloctaethylchlorin.
[c]2,4-Dimethyloctaethylisobacteriochlorin.
[d]tw = this work.
[e]Determined by spectroelectrochemistry.

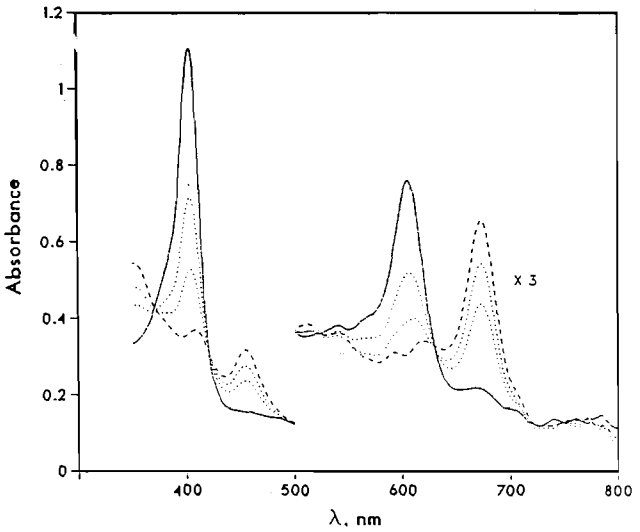

Fig. 3. Thin-layer spectroelectrochemistry of Fe(MOEC)(Cl) in THF at platinum gauze electrode. Solid line: Fe(MOEC); dashed line: $Fe(MOEC)^-$; dotted line: spectra generated during the reduction. Supporting electrolyte: 0.10 M TBAP.

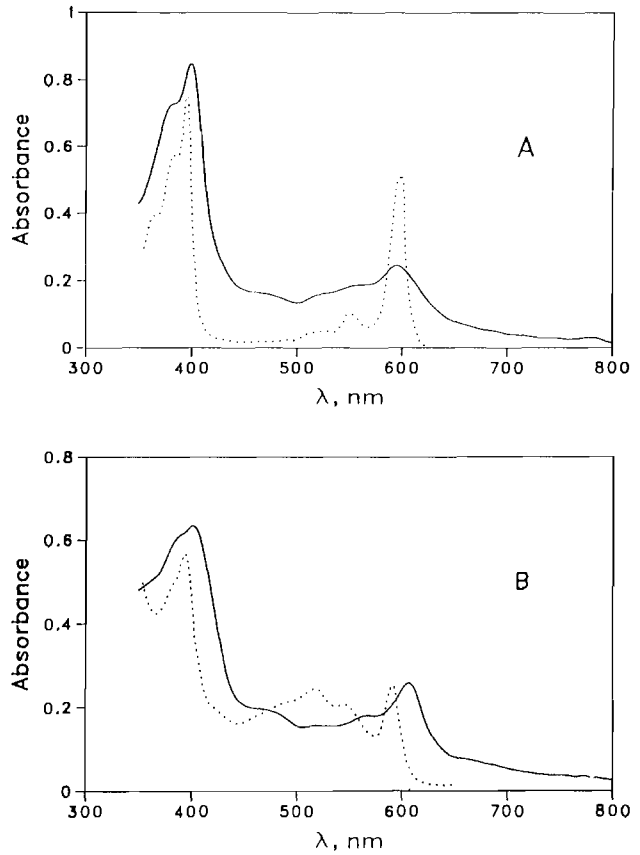

Fig. 4. (A) Solid line: visible spectrum of Fe(2,4-DMOEiBC) in THF, generated in an OTTLE cell at a platinum gauze electrode, 0.10 M TBAP. Dotted line: visible spectrum of Cu(OEiBC) in DMF from Ref. [41]. (B) Solid line: visible spectrum of $Fe(2,4\text{-}DMOEiBC)^-$ in THF, generated in an OTTLE cell at a platinum gauze electrode, 0.10 M TBAP. Dotted line: visible spectrum of $Cu(OEiBC)^-$ in DMF from Ref. [41].

and new bands at longer wavelengths. For example, the original Soret band for Fe(OEP) at 407 nm split into two bands at 374 and 403 nm, as well as a broad shoulder at 440 nm. New bands at 566 and 678 nm appeared. Likewise, the Soret band for Fe(MOEC) at 405 nm split into three bands at 355, 411 and 456 nm, with the molar absorptivity decreasing by over 50%. Three Soret bands at similar positions were observed for $Fe(OEPone)^-$. The Soret bands for $Fe(2,4\text{-}OEP\text{-}dione)^-$ were also broad, but the second and third bands, that appeared in $Fe(OEPone)^-$, were present as shoulders in this complex. In the longer wavelength region, a prominent band at 676 nm for $Fe(MOEC)^-$ replaced the ferrous band at 607 nm. The same type of spectral change was observed for $Fe(OEPone)^-$ (594 to 645 nm). For $Fe(2,4\text{-}OEPdione)^-$, the shift was in the opposite direction going from 600 to 580 nm, though a broad, weak band appeared at about 700 nm.

By contrast, the changes for $Fe(2,4\text{-}DMOEiBC)^-$ were much more subtle and much less dramatic (Fig. 4). The Soret band shifted slightly from 401 to 402 nm, and the molar absorptivity decreased by only 14%, and was only slightly less than the molar absorptivity of the ferric complex. But, the molar absorptivity of $Fe(2,4\text{-}DMOEiBC)^-$ (89 mM^{-1} cm^{-1}) was not drastically different from the values of $Fe(OEP)^-$ (59 mM^{-1} cm^{-1}) and $Fe(MOEC)^-$ (108 mM^{-1} cm^{-1}). There were no new Soret bands, nor were the Soret bands significantly broader than in the ferrous spectrum.

Comparisons of iron(I) isobacteriochlorin with other metal(I) isobacteriochlorin complexes were also quite interesting. For example, the visible spectrum for $Fe(2,4\text{-}DMOEiBC)^-$ is similar to $Cu^I(OEiBC)^-$ in both the multiplicity and relative intensities of the bands [41] (see Fig. 4 and Table 4). On the other hand, the bands for the iron complex are much broader, which is typical for iron porphines, and shifted due to the presence of a different metal. Reduction of Fe(2,4-DMOEiBC) caused a small red shift in the Soret and Q (long wavelength) bands, which compared with a small blue shift in the Q band for $Cu(OEiBC)^-$. Larger blue shifts were observed in $Ni^I(OEiBC)^-$, which was interpreted to be due to extensive d_π to e_g*-like backbonding. The small changes upon reduction of Fe(2,4-DMOEiBC) would indicate weak backbonding (as in the copper case), and the small red shift could be due to destabilization of the a_{1u}-like orbital due to the addition of an electron to the d_{z^2} orbital, which has electron density in the x–y plane. Such destabilization is expected when the electron is added to a $d_{x^2-y^2}$ orbital [41].

The structure of $Fe(TPP)^-$ has been interpreted as an iron(I) complex with significant backbonding of the d_π orbitals into the porphyrin e_g* system. This backbonding would stabilize the iron(I) complex. In the alkyl isobacteriochlorin case, the e_g*-like orbital has been raised in energy which would reduce backbonding

Table 4
Visible spectra of iron porphyrin, hydroporphyrin, porphinone and porphindione complexes

Complex	Solvent	Soret bands (nm)	Other visible bands (nm) (ϵ (cm^{-1} $M^{-1}\times10^{-3}$))	Ref.
Fe(OEP)	THF	407 (122)	531 (1.24), 557 (13.6)	tw[a]
Fe(OEC)	benzene	393 (90.3)	498 (9.2), 626 (23.3)	[21]
Fe(MOEC)	THF	405 (231)	607 (49)	tw
Fe(OEiBC)	benzene	315s, 339s, 370 (31.7), 387 (33.6)	487s, 517s, 544s, 573 (10.3), 616 (21.1)	[21]
Ni(OEiBC) (high spin)	DMF	380, 400, 407	552, 594	[41]
Cu(OEiBC)	DMF	380, 392	524, 550, 594	[41]
Zn(OEiBC)	DMF	372, 394, 402	534, 594, 597	[41]
Fe(2,4-DMOEiBC)	THF	383 (103)	401 (115), 522s, 555s, 594 (33)	tw
Fe(OEPone)	THF	399s, 413 (76.7)	486s, 545 (11.0), 594 (17.6), 661 (6.0)	tw
Fe(2,4-OEPdione)	THF	394 (48)	435 (57), 523s, 600 (20)	tw
$Fe(MOEC)Cl^+$	THF	386 (159)	471 (31), 521 (25), 599 (20)	tw
$Fe(OEC)(NO)^+$	CH_2Cl_2	385	470s, 615	[42]
$Fe(2,4\text{-}DMOEiBC)(Cl)^+$	THF	386 (59)	594 (22)	tw
$Fe(OEiBC)(NO)^+$	CH_2Cl_2	380	465s, 602	[42]
$Fe(OEPone)Cl^+$	THF	396 (100)	460 (13.9), 482 (13.2), 527 (11.7), 590s (7.6)	tw
$Fe(2,4\text{-}OEPdione)(Cl)^+$	THF	390 (59)	463s (24), 520 (17)	tw
$Fe(OEP)^-$	THF	374 (59.3), 403 (45.3)	494 (12.8), 523 (11.8), 566 (13.5), 678 (4.0)	tw
$Fe(MOEC)^-$	THF	355 (108), 411 (74)	456 (64), 676 (44)	tw
$Ni(OEiBC)^-$	DMF	380	504, 532, 572	[41]
$Cu(OEiBC)^-$	DMF	380, 392	518, 548, 590	[41]
$Zn(OEiBC)^-$	DMF	400, 412	557, 600	[41]
$Fe(2,4\text{-}DMOEiBC)^-$	THF	402 (89)	568 (24), 607 (35)	tw
$Fe(OEPone)^-$	THF	364 (48.9), 407 (48.1)	446 (41.1), 522 (11.5), 585 (10.7), 645 (14.2)	tw
$Fe(2,4\text{-}OEPdione)^-$	THF	388 (43), 425s	465s, 522 (15), 580 (29)	tw

[a]tw = this work.

and destabilize the complex. This destabilization would raise the $E_{1/2}$ value when compared to the porphyrin complex. Significant changes in the redox potential upon changing the complex from OEP to OEiBC were not observed for nickel and copper, probably due to the fact that the structure of the complexes changed ($Cu^{II}(OEP^-)$ versus $Cu^{I}(OEiBC)^-$) [41]. Such changes would not be expected for iron because iron(I) is formed with porphyrin itself.

The first oxidation of Fe(MOEC)(Cl), Fe(2,4-DMOEiBC)(Cl), Fe(OEPone)(Cl) and Fe(2,4-OEPdione)(Cl) was examined by OTTLE visible spectroelectrochemistry. The oxidation of Fe(MOEC)(Cl) and Fe(2,4-DMOEiBC)(Cl) (Fig. 5) was characterized by small changes in the Soret band molar absorptivity, with a red shift for the chlorin complex. In both cases, the band at 600 nm was attenuated (chlorin) or disappeared (isobacteriochlorin). Similar spectral changes were observed when the siroheme in *E. coli* sulfite reductase was oxidized to the superoxidized state by porphyrexide [44] (see insert, Fig. 5). The formation of π-cation radicals from $Fe^{II}(OEC)(NO)$ and $Fe^{II}(OEiBC)(NO)$ lead to spectra that were quite similar

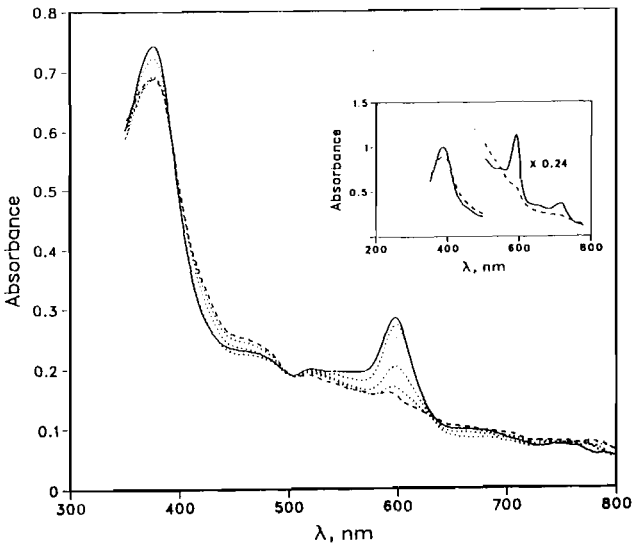

Fig. 5. Thin-layer spectroelectrochemistry of Fe(2,4-DMOEiBC)(Cl) in THF at a platinum gauze electrode. Solid line: Fe(2,4-DMOEiBC)(Cl) in THF; dashed line: $Fe(2,4\text{-}DMOEiBC)(Cl)^+$; dotted line: spectra generated during the oxidation. Supporting electrolyte: 0.10 M TBAP. Insert: visible spectrum of 15.1 μM *E. coli* sulfite reductase before (solid line) and after (dashed line) addition of 1.25 equiv. of porphyrexide at 5 °C [44].

to Fe^{III}(MOEC)(Cl)$^+$ and Fe^{III}(2,4-DMOEiBC)(Cl)$^+$, respectively (see Table 4 and Fig. 1 of Ref. [42]). In particular, the bands around 600 nm are bleached significantly in both π-cation radicals, while the Soret band is only slightly affected. Direct comparison of Fig. 5 in this article with Fig. 1a in Ref. [42] shows only minor differences in the spectra, with some of the band shifts being attributed to solvent and macrocycle substitution differences. The oxidation state of the iron had little effect on the visible spectra of these π-cation radicals. As in the voltammetry, there was no evidence for macrocycle dehydrogenation, as was observed for the phenyl derivatives [11].

For the porphinone and porphindione complexes, the spectra of the π-cation radicals mirrored the results for the hydroporphyrin complexes. The oxidation led to a sharpening of the Soret band for Fe(OEPone)(Cl) and Fe(OEPdione)(Cl). In the latter case, the two Soret bands collapsed into a single band upon oxidation. The molar absorptivity of Soret band for Fe(OEPone)(Cl)$^+$ increased substantially over the neutral ferric complex. For both of these complexes, there was substantial bleaching of the bands around 600 nm, as was observed for the hydroporphyrin complexes. Overall, the spectra of the oxidized species for the hydroporphyrin, porphinone and porphindione ferric complexes were consistent with the formation of π-cation radical complexes.

3.3. Electrochemical studies of pyridine coordination to iron hydroporphyrins

The addition of pyridine into a THF solution of iron hydroporphyrin resulted in a new reversible wave (wave Ib), which appeared at a potential less negative than the original reduction wave (wave Ia). As the concentration of pyridine increased, this new wave (wave Ib) increased at the expense of the original first wave, and eventually replaced the original wave at high concentrations of pyridine. This behavior has been observed for other iron porphyrin complexes [11,25,45]. The ratio of the ferric/ferrous bis(pyridine) formation constants were calculated on the basis of the shift in the half-wave potential of the first wave (Eq. (2)). The individual β_2 values were calculated from the shift in the half-wave potential of the second wave using Eq. (1). Because the shift in half-wave potentials corresponded to Eq. (1), there was no evidence for coordination of iron(I) with pyridine. The log β_2 results for pyridine and substituted pyridines are shown in Table 5, along with their variation as a function of the pK_a of the substituted pyridine base.

For the ferric complexes, there was good linearity for all the plots of log β_2^{III} versus pK_a with the relative standard deviations of the slopes being less than 10% for all the complexes. The changes in the formation constants of ferric porphines with substituted pyridines as a function of the pK_a of the base were consistent with previous work [25,45]. There was no statistical difference in the slopes of the log β_2^{III} versus pK_a plots for the different macrocycles. Unlike the slopes, though, the intercepts for the ferric methylated hydroporphyrin complexes increased on going from the porphyrin to chlorin to isobacteriochlorin macrocycle. Thus, the β_2^{III} values for Fe(MOEC)(py)$_2^+$ and Fe(2,4-DMOEiBC)(py)$_2^+$ were 9 ± 5 and 80 ± 2 times larger than the β_2^{III} value for Fe(OEP)(py)$_2^+$. This result confirms the tentative results obtained for the phenyl hydroporphyrins [11]. In contrast to the ferric complexes, there was no systematic relationship between the pK_a values of the ferrous hydroporphyrins and the pyridine pK_a. This lack of linearity has been observed before [25], and has been rationalized on the basis of competition between σ and π bonding in the ferrous–pyridine complex [25]. A linear relationship between the log β_2^{II} and pK_a values should be observed if the metal–ligand bond is dominated by σ bonding. In comparing the formation constants for a given ligand, there was no systematic increase in the log β_2^{II} values with increased saturation of the macrocycle.

Table 5
Formation constants[a] for pyridine complexes with iron porphines

Pyridine	pK_a	log β_2^{II}/log β_2^{III}		
		Fe(OEP)(Cl)[b]	Fe(MOEC)(Cl)[c]	Fe(2,4-DMOEiBC)(Cl)[d]
3-Cyanopyridine	1.40	4.69/−4.04	5.70/−3.75	6.06/−1.56
Acetylpyridine	3.18	6.02/−2.12	6.79/−0.86	6.42/−0.50
Pyridine	5.28	5.37/1.27	6.35/1.30	6.87/3.24
Lutidine	6.46	5.39/1.36	6.49/3.27	6.18/3.25
4-DMAP[e]	9.71	6.43/4.91	7.12/5.63	7.18/6.64

[a]Formation constants for reactions (3) and (4).
[b]Slope of log β_2^{II} vs. pK_a = 0.15 ± 0.08; slope (intercept) of log β_2^{III} = 1.1 ± 0.1 (-5.3 ± 0.6).
[c]Slope of log β_2^{II} vs. pK_a = 0.13 ± 0.06; slope (intercept) of log β_2^{III} = 1.1 ± 0.1 (-4.7 ± 0.7).
[d]Slope of log β_2^{II} vs. pK_a = 0.11 ± 0.06; slope (intercept) of log β_2^{III} = 1.0 ± 0.1 (-3.1 ± 0.7).
[e]4-DMAP = 4-(dimethylamino)pyridine.

4. Conclusions

The visible spectra of a number of important iron hydroporphines, porphinone and porphindiones in various oxidation states have been reported. The visible spectra of most of the FeP^- complexes were similar in that the Soret band was attenuated upon reduction of the ferrous complex, and the number of bands increased. This attenuation was least pronounced in the case of Fe(2,4-DMOEiBC)$^-$. In addition, there was no increase in the multiplicity of Soret bands. These changes mimic those reported for Fe(TPiBC)$^-$ [11]. The changes in the visible spectrum upon oxidation were quite similar with a bleaching of the long wavelength bands, along with changes in the Soret band(s). These changes were typical of the formation of a π-cation radical complex. When these spectra were compared with $Fe^{II}(NO)(P^{\cdot+})$ complexes [42], the oxidation state of the iron had little effect on the visible spectra.

Finally, the β_2^{III} values for the iron pyridine complexes confirm the results previously estimated for the tetraphenyl substituted complexes [11]. An increase in Lewis acidity of the ferric porphine complex was observed as the macrocycle became more saturated. No changes in Lewis acidity of the ferrous complexes were observed, which may be due to a complex relationship between σ and π bonding between the iron and pyridines. Poor linearity of the log β_2^{II} values versus the pK_a of the pyridine ligand, which is indicative of π interactions between the iron and the ligand, was observed for the ferrous complexes.

The redox potentials for FeP/FeP^- were relatively independent of macrocycle identity except for the 2,4-DMOEiBC complex. Inductive effects alone cannot rationalize the 300–400 mV negative shift in these two half-wave potentials. In addition, these shifts closely correspond to the difference in redox potentials between the free-base porphyrin and isobacteriochlorin ligands. These shifts are probably due to changes in the extent of backbonding between the metal and the macrocycle, which may stabilize the iron(I) complex [40]. Work is in progress in our laboratory in order to further clarify the oxidation state and reactivity of the Fe(2,4-DMOEiBC)$^-$ complex.

References

[1] J.A. Cole and S.J. Ferguson (eds.), *The Nitrogen and Sulfur Cycles, 42nd Symp. Society for General Microbiology, New York, 1988,* Cambridge University Press, Cambridge, UK, 1988.

[2] M.J. Murphy, L.M. Siegel, S.R. Tove and H. Kamin, *Proc. Natl. Acad. Sci. U.S.A., 71* (1974) 612.

[3] E.T. Adman, M.W. Mather and J.A. Fee, *Biochim. Biophys. Acta, 1142* (1993) 93.

[4] C.K. Chang, *J. Biol. Chem., 260* (1985) 9520.

[5] C.K. Chang, L.K. Hanson, P.F. Richardson, R. Young and J. Fajer, *Proc. Natl. Acad. Sci. U.S.A., 78* (1981) 2652.

[6] C.K. Chang and J. Fajer, *J. Am. Chem. Soc., 102* (1980) 848.

[7] E. Fujita and J. Fajer, *J. Am. Chem. Soc., 105* (1983) 6743.

[8] C.K. Chang, K.M. Barkigia, L.K. Hanson and J. Fajer, *J. Am. Chem. Soc., 108* (1986) 1352.

[9] E.P. Sullivan, Jr. and S.H. Strauss, *Inorg. Chem., 28* (1989) 3093.

[10] D. Melamed, E.P. Sullivan, Jr., K. Prendergast, S.H. Strauss and T.G. Spiro, *Inorg. Chem., 30* (1991) 1308.

[11] I.-K. Choi and M.D. Ryan, *New J. Chem., 16* (1992) 591.

[12] W. Flitsch, *Adv. Heterocycl. Chem., 43* (1988) 73.

[13] H. Scheer, in D. Dolphin (ed.), *The Porphyrins,* Vol. 2, Academic Press, New York, 1978.

[14] C.K. Chang and C. Sotiriou, *J. Org. Chem., 50* (1985) 4989.

[15] C.K. Chang, C. Sotiriou and W. Wu, *J. Chem. Soc., Chem. Commun.,* (1986) 1213.

[16] C.K. Chang, *Biochemistry, 19* (1980) 1971.

[17] A.M. Stolzenberg, S.H. Strauss and R.H. Holm, *J. Am. Chem. Soc., 103* (1981) 4763.

[18] H.W. Whitlock, J.R. Hanauer, M.Y. Oester and B.K. Bower, *J. Am. Chem. Soc., 91* (1969) 7495.

[19] A.M. Stolzenberg, P.A. Glazer and B.M. Foxman, *Inorg. Chem., 25* (1986) 983.

[20] G. Peychal-Heiling and G.S. Wilson, *Anal. Chem., 43* (1971) 550.

[21] A.M. Stolzenberg, L.O. Spreer and R.H. Holm, *J. Am. Chem. Soc., 102* (1980) 364.

[22] G.A. Heath, M.R. Low, R.C.S. McQueen and A. Pelter, *J. Chem. Soc., Perkin Trans. 2,* (1984) 305.

[23] S.H. Strauss and R.G. Thompson, *J. Inorg. Biochem., 27* (1986) 173.

[24] P.F. Richardson, C.K. Chang, L.D. Spaulding and J. Fajer, *J. Am. Chem. Soc., 101* (1979) 7736.

[25] D. Feng, Y.-S. Ting and M.D. Ryan, *Inorg. Chem., 24* (1985) 612.

[26] D. Lexa, J.-M. Saveant and D.L. Wang, *Organometallics, 5* (1986) 1428.

[27] T. Mashiko, C.A. Reed, K.J. Haller and W.R. Scheidt, *Inorg. Chem., 23* (1984) 3192.

[28] A.M. Stolzenberg and L.J. Schussel, *Inorg. Chem., 30* (1991) 3205.

[29] M.W. Renner, L.R. Furenlid, K.M. Barkigia, A. Forman, H.-K. Shim, D.J. Simpson, K.M. Smith and J. Fajer, *J. Am. Chem. Soc., 113* (1991) 6891.

[30] P.A. Connick and K.A. Macor, *Inorg. Chem., 30* (1991) 4654.

[31] K.A. Macor, R.S. Czernuszewicz and T.G. Spiro, *Inorg. Chem., 29* (1990) 1996.

[32] R.S. Czernuszewicz, K.A. Macor, X.Y. Li, J.R. Kincaid and T.G. Spiro, *J. Am. Chem. Soc., 111* (1989) 3860.

[33] X.Q. Lin and K.M. Kadish, *Anal. Chem., 57* (1985) 1498.

[34] K.M. Kadish, L.A. Bottomley and J.S. Cheng, *J. Am. Chem. Soc., 100* (1978) 2731.

[35] D. Lexa, P. Rentien, J.-M. Saveant and F. Xu, *J. Electroanal. Chem., 191* (1985) 253.

[36] I.-K. Choi, *Ph.D. Thesis,* Marquette University, Milwaukee, WI, 1989.

[37] A.M. Stolzenberg and M.T. Stershic, *J. Am. Chem. Soc., 110* (1988) 6391.

[38] A. Giraudeau, H.J. Callot, J. Jordan, I. Ezhar and M. Gross, *J. Am. Chem. Soc., 101* (1979) 3857.

[39] A. Giraudeau, A. Louati, M. Gross, H.J. Callot, L.K. Hanson, R.K. Rhodes and K.M. Kadish, *Inorg. Chem., 21* (1982) 1581.

[40] R.J. Donohoe, M. Atamian and D.F. Bocian, *J. Am. Chem. Soc., 109* (1987) 5593.
[41] A.D. Procyk, A.M. Stolzenberg and D.F. Bocian, *Inorg. Chem., 32* (1993) 627.
[42] S. Ozawa, H. Fujii and I. Morishima, *J. Am. Chem. Soc., 114* (1992) 1548.
[43] C.A. Reed, in K.M. Kadish (ed.), *Electrochemical and Spectrochemical Studies of Biological Redox Components,* American Chemical Society, Washington, DC, 1982, p. 333.
[44] L.J. Young and L.M. Siegel, *Biochemistry, 27* (1988) 5984.
[45] K.M. Kadish and L.A. Bottomley, *Inorg. Chem., 19* (1980) 832.